

Trigger strategies for central exclusive $H \rightarrow b\bar{b}$ studies with the AFP detector

G. J. A. Brown¹, M. Campanelli², A. Kupco³, A. D. Pilkington¹, M. Tasevsky³

¹ *School of Physics and Astronomy, University of Manchester, Manchester, M13 9PL, UK*

² *Department of Physics and Astronomy, University College London, London, WC1E 6BT, UK.*

³ *Institute of Physics of the AS CR v.v.i., Na Slovance 2, CZ-182 21 Praha 8, Czech Republic.*

Abstract



The ATLAS Forward Proton (AFP) upgrade proposes to install proton detectors at 220 m and 420 m either side of the ATLAS interaction point, turning the LHC into a giant magnetic spectrometer. The physics motivation for this upgrade focuses on final states in which the colliding protons remain intact, allowing a full reconstruction of the event, even in the forward region. One such process is the production of the Higgs boson in the central exclusive channel and tagging the outgoing protons allows the possible extraction of the Higgs quantum numbers, mass and couplings regardless of the decay channel. The locations of these proton detectors are determined by the accelerator components and lattice, but the combination of the two covers quite a wide mass range for the central system. Studying this exclusive production channel for the presently favoured low Higgs mass depends on the possibility of efficiently triggering, up to the highest luminosities, on a pair of relatively soft jets coming from the decay of b quarks or τ leptons. As jet triggers will inevitably be heavily pre-scaled, even at modest luminosities, it is essential to make a coincidence between information from the tagging detectors and the central system as early as possible at Level 1. In this note, we describe some possible solutions that result in an efficient low-mass $H \rightarrow b\bar{b}$ trigger with AFP.

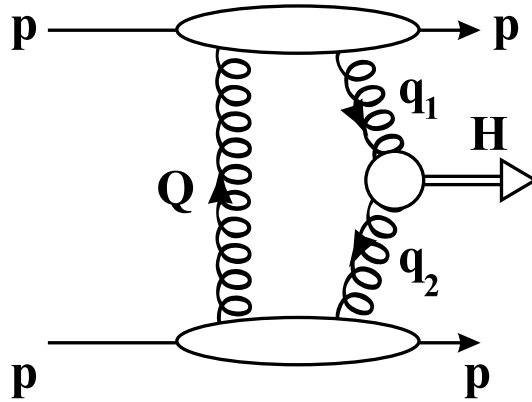


Figure 1: The central exclusive production of Higgs bosons at the LHC.

1 Introduction

The importance of the central exclusive production (CEP) mechanism to study the Higgs boson properties has been already discussed in many dedicated papers [1, 2, 3, 4]. The Higgs boson is produced by gluon-gluon fusion, but the protons remain intact due to the presence of a screening gluon as shown in Figure 1. The final state therefore consists of a Higgs boson, two outgoing protons and no other hadronic activity. Only scalar particles can be produced as resonances in this channel. We do not go into further details, but remark that this channel has often been described as the possibility of performing at the LHC some of the measurements only believed possible at a future Linear Collider.

It is also worth mentioning that, although central exclusive Higgs production cannot be considered as a discovery channel due to the larger luminosity required with respect to more standard channels, the mass measurement obtained could be much better. In this case, the Higgs mass would be calculated from the very well measured momentum of the two protons detected in the AFP detectors, exploiting the fact that the Higgs boson is produced *exclusively*. The AFP proposal is to build four tracking stations located at 220 m and 420 m on both sides of the ATLAS interaction point (IP). The detectors will be capable of measuring both the position of a proton with respect to the beam and the time-of-flight of each proton from the interaction point. Further details regarding the AFP detector can be found in [4]. Finally, it should be noted that, in addition to precision Higgs boson measurements, there is a wide range of electroweak physics studies possible with the AFP detectors. These include anomalous gauge boson couplings and supersymmetry measurements and can be studied using standard ATLAS leptonic triggers.

In this note, we determine a trigger strategy to retain central exclusive $H \rightarrow b\bar{b}$ events. As we will see in the following, the knowledge of the approximate value of the Higgs mass can be used to reduce the rates at trigger level, keeping good efficiency for the signal. The layout of the note is as follows: In section 2, the ATLAS Level 1 (L1) calorimeter trigger system is discussed, both in relation to its present configuration and proposed upgrade. In section 3, the L1 trigger capability of the proposed AFP detectors at 220m will be discussed. In section 4, the trigger efficiency for signal events is discussed. Finally in section 5, the background rates for a variety of trigger strategies are presented.

2 The ATLAS L1 Calo system: present configuration and proposed upgrades

The ATLAS L1 Calorimeter trigger is composed of a central region, plus two forward-backward regions. Central and forward calorimeters are seen by the system as two independent detectors. The boundary between the central-forward regions is set at a pseudo-rapidity value of 3.2, i.e. the physical boundary between the forward calorimeter (FCAL) and the hadronic endcap.

At present, jets are reconstructed in towers of 0.8×0.8 in the $\eta - \phi$ plane. However, detailed information (E_T , η , ϕ) is not propagated to the central trigger processor (CTP) for bandwidth occupancy reasons and therefore cannot be used for the trigger decision. The only information currently available to define L1 jet trigger items is the number of jets passing a given transverse energy threshold (separately for the central and forward regions). For the 2009-2010 data taking, to keep the system as simple as possible, it was decided that only inclusive single jet signatures are used - the only exception is the forward di-jet (2FJ18) trigger that requires two jets in the forward calorimeters above an E_T threshold of 18 GeV.

At the time of the AFP detector installation, a substantial upgrade of the L1 calorimeter trigger system is likely to be operational [5]. The main improvement would be an increase of the bandwidth, allowing the use of the E_T and topological information of each individual jet in the L1 processing. The processing itself would require a new *global merger* processor, which would allow the definition of new trigger quantities based on the leading jets in the event. This new processor is foreseen to be part of the trigger upgrade and we will present trigger rates that utilize this topological information in section 5. It is also foreseen that the granularity would be improved by a factor two and so it is likely that η and ϕ information for each jet will be available in discrete values of size 0.4×0.4 . Finally, quantities such as di-jet mass could be calculated using the global merger processor. We do not consider such an option in this note, but draw attention to the fact that this could allow a further reduction in the L1 rate. It is likely that the increased amount of information we are planning to process in the CTP following this upgrade will also result in an increased processing time, therefore possibly more dead time, especially in the electromagnetic calorimeter. This issue is presently under study.

3 Trigger considerations for the detector station at 220 m

The jet (and di-jet) L1 trigger items will be heavily pre-scaled even at moderate instantaneous luminosities. In order to keep a relatively high efficiency for the Higgs search, we need to impose a coincidence between the two jets in the central region and a tagged proton in the forward detector. To get the best mass resolution, we have to require also that the other proton is detected in the opposite side in the 420 m station (for the light Higgs case), but unfortunately this detector is too far to be included in the Level 1 trigger information. In fact, the maximum value of the L1 latency for a complete trigger decision is 2500 ns^1). This means that the signal from each sub-detector has to reach the CTP within 1900 ns, since about 600 ns are needed to take a decision and propagate it to the various sub-detector systems. The time-of-flight of the proton from the interaction point to the 420 m station, plus the time it would take for a signal, even travelling at the speed of light, to reach the CTP is much larger than the 1900 ns limit. On the other hand it is, in principle, possible to trigger on protons tagged in the detector stations at 220 m from the interaction point. The present baseline design for the 220 m

¹⁾The current latency is somewhat smaller than this.

trigger system foresees the use of a quartz bar detector, shaped to optimize signal/background rejection, read out by an optical fibre. The fibre would be read out by an MCP photomultiplier, amplified, and the signal accepted if it passes the threshold of a constant fraction discriminator. After a local coincidence logic, the signal would be sent to the CTP using an air-core cable similar to what is used by the ALFA detector [6]. Details of the proposed system are discussed in a separate note [7].

The main contribution to the L1 rate for our *di-jet plus proton* trigger comes from the coincidence, in the same bunch crossing, of a di-jet event and an event that produces a forward proton, mainly coming from single-diffractive or non-diffractive scattering, within the AFP acceptance.

The probability that in N proton-proton interactions there are k events producing a forward proton is a binomial,

$$B(N, k) = \binom{N}{k} (2\varepsilon)^k (1 - 2\varepsilon)^{N-k}, \quad (1)$$

where ε is the fraction of events at the LHC that have a forward proton within the acceptance of the 220 m detector station. A proton is observed for $k \geq 1$, so the probability of a proton ‘hit’ at 220 m is given by

$$B(N) = \sum_{k=1}^N B(N, k) = 1 - (1 - 2\varepsilon)^N, \quad (2)$$

which is valid for exactly N interactions. Assuming that there are, on average, μ interactions per bunch crossing, the probability of a forward proton within the acceptance of the detector stations at 220 m is

$$P = \sum_{N=0}^{\infty} P_{\mu}(N) B(N) = 1 - e^{-2\mu\varepsilon} \quad (3)$$

where $P_{\mu}(N)$ is the poisson distribution, i.e.

$$P_{\mu}(N) = \frac{\mu^N}{N!} e^{-\mu}. \quad (4)$$

If we also require that a hard scatter is present, we have to replace $P_{\mu}(N)$ with

$$P'_{\mu}(n) = \frac{P_{\mu}(N+1)}{P_{\mu}(1+)} \quad (5)$$

In the end the combined probability of having a tagged proton and a hard event is

$$P' = 1 - \frac{1}{1 - \varepsilon} \frac{e^{-\varepsilon\mu} - e^{-\mu}}{1 - e^{-\mu}}. \quad (6)$$

Note that a change in the expected value of μ can have a large effect on the probability of having a hard scatter and a forward proton tag in the same bunch crossing. This means that the rate of a trigger based on a forward proton at 220 m from the IP has more than a linear dependence on the average number of interactions in each bunch crossing, and hence the luminosity.

The key to reducing this background in the L1 trigger is to reduce ε , i.e. the acceptance of generic forward protons, without overly affecting the signal efficiency. For a given Higgs mass, it is possible to calculate the expected distribution of momentum lost by the two protons. This can be easily translated into the $x - y$ distribution of the protons in the forward detector stations at 220 m. In particular, for the most difficult case of light Higgs masses, the lost momentum will be quite small; either both protons will be tagged in the detector stations at 420 m from the IP (which is impossible to trigger on, as discussed earlier), or one will be tagged at 420 m and one at 220 m. For the latter case, the $x - y$

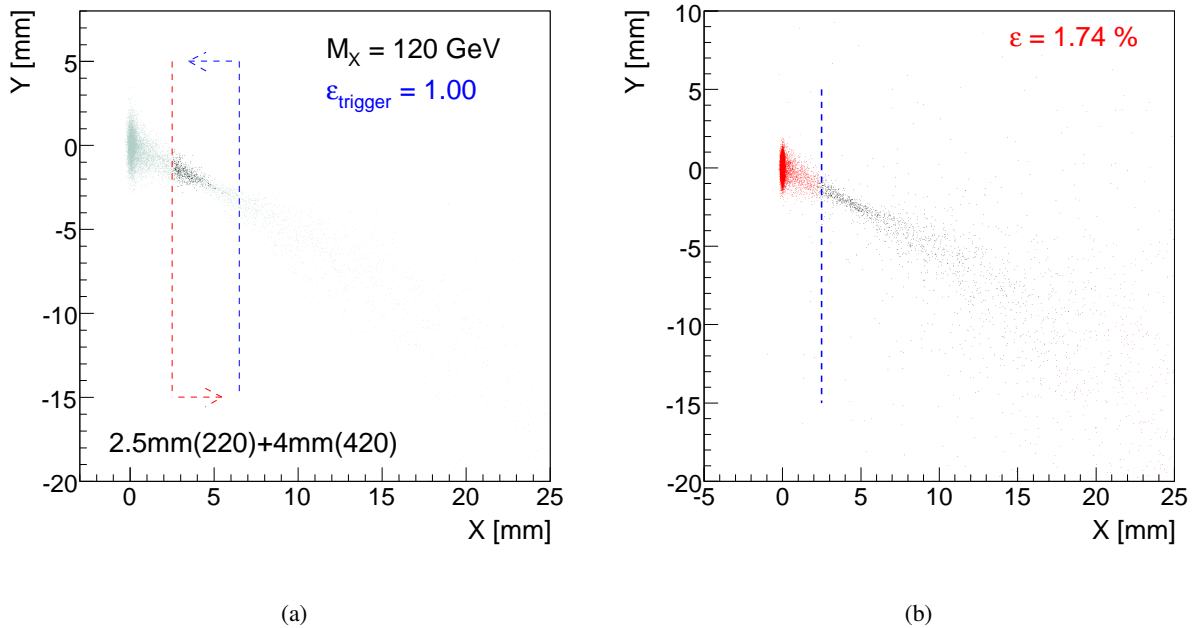


Figure 2: The $x - y$ distribution of protons tagged in the detector stations at 220 m from the IP for exclusive Higgs mass of 120 GeV given that a proton is also present in a detector at 420 m on the other side (a). The corresponding plot for all events at the LHC is shown in (b). Protons are tracked through the LHC lattice using MAD-X [8] and cross-checked with FPTrack [9]. The dashed lines represent the acceptance limits of the detector.

distribution of protons from exclusive Higgs events ($m_H = 120$ GeV) in the detector station at 220 m is shown in Figure 2 (a). Signal protons are concentrated in the inner part of the detector i.e. within 4 mm of the detector edge. As we can see from Figure 2 (b), the background protons, which determine the L1 trigger rate, are spread over a larger distance. It has been calculated using events simulated by PYTHIA that the occupancy in the detector stations at 220 m drops by a factor of two simply by requiring that the protons lie within the 4 mm of the detector edge. The x distributions for different values of the Higgs mass are shown in Figure 3. It is clear that the majority of asymmetric events can be retained by triggering only on protons that are tagged on the inner side of the detector at 220 m.

In the subsequent sections, we assume that the detectors stations at 220 m will have an active detector edge 2.5 mm from the beam, and that the final design of the detector stations at 220 m will allow us to select events in which the proton is tagged in the innermost 4 mm of the detector. With these assumptions, the L1 rejection obtained by requiring a forward proton at 220 m ranges from approximately 14 at a luminosity of $2 \times 10^{33} \text{ cm}^{-2} \text{ s}^{-1}$, to 5 at $5 \times 10^{33} \text{ cm}^{-2} \text{ s}^{-1}$ and about 3 at $10^{34} \text{ cm}^{-2} \text{ s}^{-1}$.

4 Trigger efficiency for signal

Figures 4 (a) and 4 (b) show the jet trigger efficiency as a function of the leading jet's transverse energy for inclusive and exclusive dijet events respectively. The inclusive samples are fully simulated PYTHIA [10] di-jet events and the exclusive sample is fully simulated Higgs signal events by

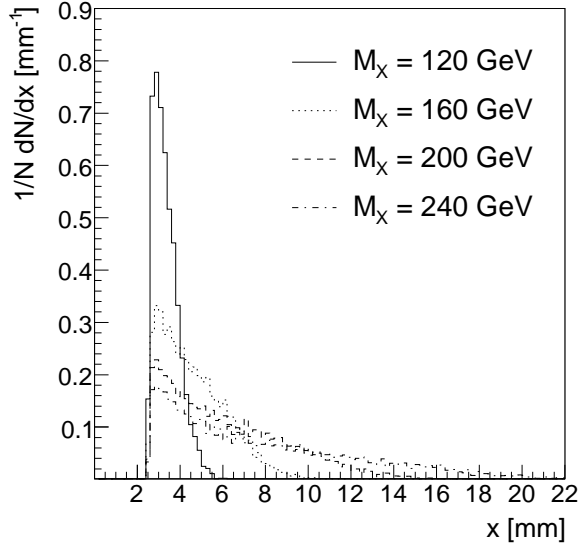


Figure 3: The x distribution of protons detected at 220 m from exclusive Higgs events of different mass, given that the other proton is tagged in the detector station at 420 m on the other side of the IP.

ExHuME [11], a generator explicitly designed for central exclusive final states. See Appendix A for details on the generated samples. The trigger items are 2J35 (jets are central, $|\eta| < 3.2$, with $E_T > 35$ GeV), J35+J23 (one jet with $E_T > 35$ GeV and the other with $E_T > 23$ GeV) and 2J42 (both with $E_T > 42$ GeV). Since in the process of writing this note, a proposal to round-off the thresholds has been made, we will also show some rates for a J40 + J20 configuration, to show that even this new trigger configuration will not change radically the results of this study.

We can see that the ‘softest’ di-jet threshold (J35+J23) is the only one that can give a reasonable efficiency for jets coming from light Higgs decays, with transverse energies of the order of 50-60 GeV. Keeping this result in mind, we now examine the rates of the three trigger configurations.

5 Expected rates for the various trigger configurations

We estimate the jet trigger rates using fully-simulated PYTHIA di-jet events and cross check the estimate using PYTHIA minimum bias (non-diffractive) events. A list of samples are given in Appendix A. Due to the lack of samples with pile-up, these numbers do not account for the added hadronic activity due to multiple proton-proton interactions in the same bunch-crossing. However, it can be expected that these numbers will not change too much after corrections to the trigger jet energy scale are applied for the average pileup deposit. Since the cross section in the forward region is quite uncertain, the question could arise on how reliable predictions based on Pythia are. This issue has been already discussed in several places, for instance on table 1 of [3]. The bottom line is that the diffractive forward protons have a similar rate between models (after all the form of the cross section is well known) and the difference is in the non-diffractive (reggeon exchange) rate. However, the large difference between models ($\pm 50\%$) occurs at very large ξ . We are protected from this somewhat by only triggering on events with small values of ξ . For instance, for $\xi < 0.1$ (very conservative) we have an increase of 12% (per LHC event) for the probability of forward protons given PHOJET instead of PYHTIA. For

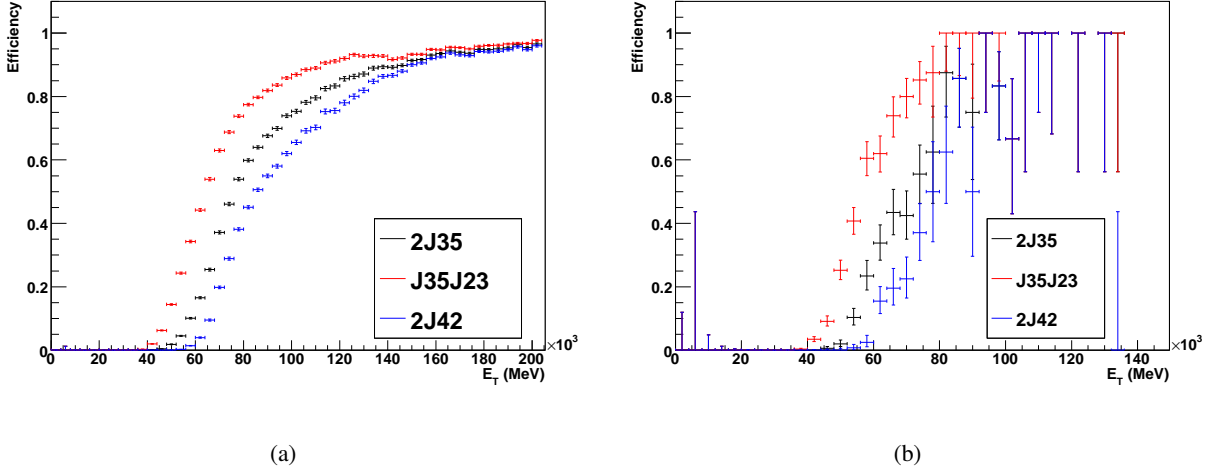


Figure 4: The trigger efficiency for the J35+J23, 2J35 and 2J42 trigger items for (a) inclusive di-jet events and (b) exclusive events.

L1 item	Rate at 2×10^{33} (kHz)	Rate at 10^{34} (kHz)
J23	370	1850
J35	97	483
J42	52	259

Table 1: The expected single jet trigger rate at ATLAS.

$\xi < 0.05$ (closer to our actual trigger) the increase in forward proton probability is smaller.

The available L1 bandwidth assigned to an AFP-based measurement of $H \rightarrow b\bar{b}$ will depend firstly on ATLAS discovery and then subsequently on the importance placed by the Collaboration on this channel - a reasonable estimate is about 2 kHz. Table 1 shows the rate of the single jet triggers and clearly these numbers would have to be heavily pre-scaled. Adding the requirement of a second jet (Table 2) does help - the J23+J35 trigger has a considerably smaller rate than the inclusive J35 trigger, whilst the efficiency for signal events is comparable. However, we are still far from the estimate for the available rate.

Let us consider now the case in which at least one forward proton is detected in the AFP detector stations at 220 m in addition to the di-jets in the central calorimeter. As discussed in section 3, rather than considering the full AFP detector acceptance we assume that the trigger can select those

L1 item	Rate at 2×10^{33} (kHz)	Rate at 10^{34} (kHz)
2J23	84	418
2J35	24	118
J23+J35	52	261
2J42	14	68
J20+J40	43	216

Table 2: The expected di-jet trigger rate at ATLAS.

L1 item	Rate at 2×10^{33} (kHz)	Rate at 10^{34} (kHz)
2J23 + p220	6.0	144
2J35 + p220	1.7	41
J23+J35 + p220	3.7	90
2J42 + p220	1.0	23
J20+J40 + p220	3.1	75

Table 3: The rate for a di-jet plus forward proton trigger. The forward proton is required to be within the first 4 mm of the detector station at 220m from the IP.

protons in the inner 4 mm (i.e. the part of the detector that is closest to the beam position). The rates for the di-jet trigger plus forward proton requirement (p220) are shown in Table 3. We see that the addition of the forward proton tag reduces the rate by a factor of approximately 14 for a luminosity of $2 \times 10^{33} \text{ cm}^{-2} \text{ s}^{-1}$, but only by a factor of ~ 3 at a luminosity of $10^{34} \text{ cm}^{-2} \text{ s}^{-1}$. It should be noted that this is the best achievable rate given the present (not upgraded) ATLAS trigger configuration plus the addition of a L1 AFP trigger.

If the L1 calorimeter trigger is upgraded as discussed in section 2, additional handles can be utilized. The first possibility is to exploit the kinematic correlations between the pseudo-rapidities of the protons and the jets. This is especially useful as pile-up should not overly affect jet directions (unlike the jet energy) and so our results should be valid at the highest luminosities. Given the information from the 220 m detector stations, we know the side of the detector the candidate exclusive proton was tagged on. For a light Higgs ($\sim 120 \text{ GeV}$), the two jets from an exclusive event will be boosted in the direction of the proton tagged in the detector station at 220 m. We can therefore utilize the average di-jet rapidity,

$$\bar{\eta} = \frac{1}{2}(\eta_1 + \eta_2), \quad (7)$$

where $\eta_{1,2}$ are the pseudo-rapidities of the two leading jets. Figure 5 (a) shows the average di-jet distribution for exclusive and inclusive di-jet events given that a proton is tagged on the A-side ($\eta > 0$) of the detector and that the J35+J23 threshold is passed. Note that the inclusive di-jet distribution is symmetric because the di-jet boost has no correlation with the proton tag. Thus we can utilize the L1 trigger requirement that

- $\bar{\eta} > X_A$ if the proton is tagged on the A-side of the detector and
- $\bar{\eta} < -X_A$ if the proton is tagged on the C-side of the detector,

where X_A is a threshold. The first two rows of Table 4 show the reduction in rate for the J23+J35 L1 di-jet trigger (plus forward proton), for values of $X_A = 0.5$ or $X_A = 1.0$. We choose the more conservative option, $X_A = 0.5$ in the remainder of the trigger discussion. At this point, the rate at a luminosity of $2 \times 10^{33} \text{ cm}^{-2} \text{ s}^{-1}$ is around the 2kHz target, but the high luminosity rate remains far too large.

Another handle we can use is the requirement that jets coming from Higgs decays are relatively collinear. Figure 5 (b) shows the difference in pseudo-rapidity between the two jets, $\Delta\eta$, given by

$$\Delta\eta = |\eta_1 - \eta_2| \quad (8)$$

for signal and background events. The distributions are shown after all previous trigger requirements. The reduction in rate for $\Delta\eta < X_D$, where X_D is threshold of 1.5 or 2.0, is shown in the final three

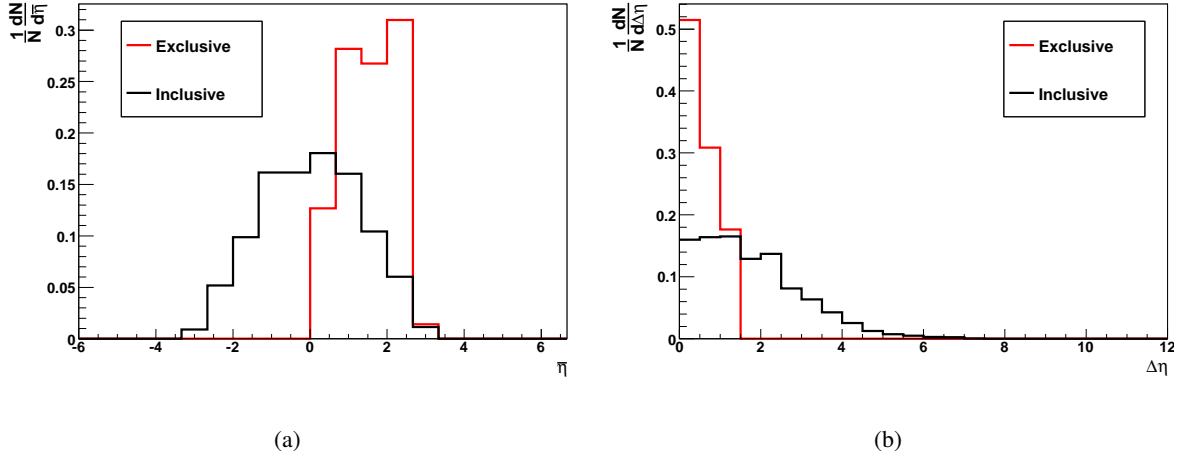


Figure 5: The average di-jet rapidity given a proton tag in the detector station at 220 m on the A-side of the detector (a). The difference in pseudo-rapidity of the two leading jets (b).

L1 item	Rate at 2×10^{33} (kHz)	Rate at 10^{34} (kHz)
J23+J35 + p220 + $X_A=0.5$	1.4	34
J23+J35 + p220 + $X_A=1.0$	1.0	23
J23+J35 + p220 + $X_A=0.5 + X_D=1.5$	0.8	19
J23+J35 + p220 + $X_A=0.5 + X_D=2.0$	1.0	23
J20+J40 + p220 + $X_A=0.5$	1.1	28
J20+J40 + p220 + $X_A=1.0$	0.8	19
J20+J40 + p220 + $X_A=0.5 + X_D=1.5$	0.7	17
J20+J40 + p220 + $X_A=0.5 + X_D=2.0$	0.6	16

Table 4: The rates of the L1 trigger for J23+J35, plus forward proton, plus requirements on the pseudo-rapidity of the L1 leading jets.

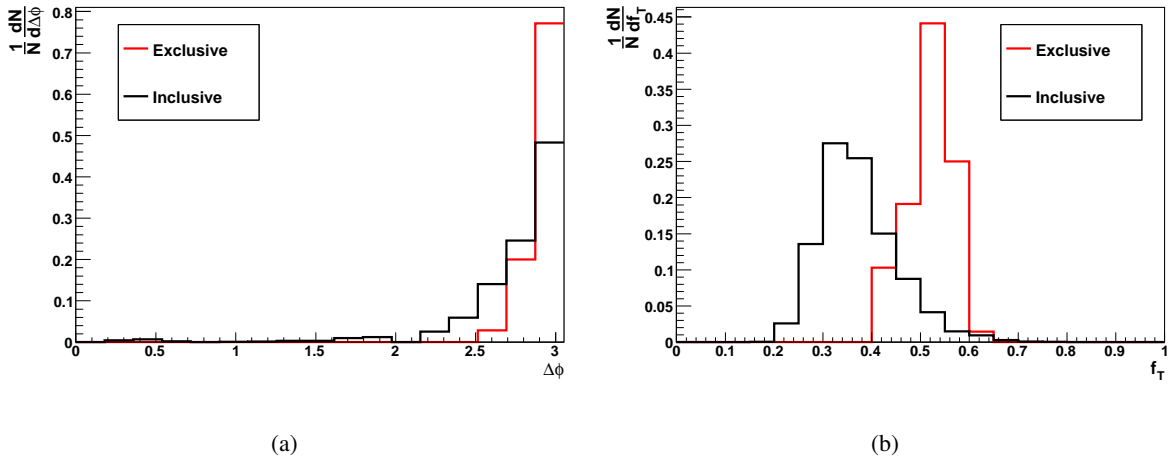


Figure 6: The difference in azimuth of the two leading jets (a). The f_T distribution (b).

rows of Table 4. We see that an additional factor of almost 2 can be gained with this cut and it is encouraging that the L1 rate is now much closer to the goal of approximately 2kHz, although a largish pre-scale would be needed at the highest luminosity. We choose the requirement $X_D < 1.5$ in the final discussion that follows.

We can make further use of the exclusivity of the event. The lack of initial state radiation in central exclusive production means that the jets are relatively back-to-back in comparison to inclusive events. Figure 6 (a) shows the azimuthal separation of the leading jets. Secondly, the lack of underlying event activity in CEP events means that the majority of energy deposited in the calorimeter will be contained within the di-jet system. We define the transverse energy fraction, f_T , as

$$f_T = \frac{E_T^1 + E_T^2}{H_T} \quad (9)$$

where $E_T^{1,2}$ are the transverse energies of the two leading jets and H_T is the total transverse energy deposited in the calorimeters. Figure 6 (b) shows the f_T distributions for signal and background events. It should be noted that the effect of pile-up on this variable could be large and is unknown due to the lack of pile-up samples. Despite this, one may expect that some separation of signal and background using f_T will still be possible at high luminosities.

Table 5 shows our final results. In the first scenario, we consider that the J35+J23 will be applied in conjunction with $X_A = 0.5$ and $X_D = 1.5$ and also that $\Delta\phi > 2.5$. In the second scenario, we consider that the J35+J23 will be applied in conjunction with $X_A = 0.5$ and $X_D = 1.5$ and also that $f_T > 0.45$. The first option is our conservative estimate as we assume that pile-up will render an f_T cut useless. The second option is our optimistic estimate, which assumes the f_T distribution will not be affected by pile-up. A realistic estimate is somewhere between the two extremes.

To put these results in context, the results published in [2, 4] assume that BSM Higgs scenarios, such as the MSSM and triplet Higgs models, can be observed with asymmetric tagging with a pre-scale of about 5. A prescale of 5 applied to the ‘conservative’ $\Delta\phi$ requirement would result in a trigger rate of approximately 2.5 to 3 kHz at $10^{34} \text{ cm}^{-2} \text{ s}^{-1}$, which is not too much above the 2kHz target rate. If however, we assume that the f_T -based trigger is applicable at the highest luminosity, we would be able to achieve the 2 kHz target using a pre-scale of around 1.5 (so, in case only integer prescales are possible, 2 or 1, depending on the actual cross section values).

L1 item	Rate at 2×10^{33} (kHz)	Rate at 10^{34} (kHz)
J23+J35 + p220 + $X_A=0.5 + X_D=1.5 + \Delta\phi > 2.5$	0.61	14.8
J23+J35 + p220 + $X_A=0.5 + X_D=1.5 + f_T > 0.45$	0.12	2.9
J20+J40 + p220 + $X_A=0.5 + X_D=1.5 + \Delta\phi > 2.5$	0.51	12.2
J20+J40 + p220 + $X_A=0.5 + X_D=1.5 + f_T > 0.45$	0.12	2.9

Table 5: The final rate estimate for the exclusivity trigger given two different final trigger requirements, $\Delta\phi$ or f_T , as explained in the text.

L1 exclusivity	Signal efficiency (%)
X_A	92 ± 9
X_D	100 ± 12
$\Delta\phi$	99 ± 12
f_T	90 ± 13

Table 6: The signal efficiency for each L1 exclusivity requirement after the events have passed the di-jet trigger and the L1 proton tag (at 220 m) requirement. The low statistics of the signal sample is reflected by the relative errors, simply estimated as $1/\sqrt{N}$ where N is the number of events passing the cut.

The signal efficiency is shown in Table 6 for each of the calorimeter based L1 trigger requirements that are imposed after the initial di-jet trigger and proton acceptance. Given the low pre-scale, it seems reasonable that a L1 trigger can be constructed to retain exclusive $H \rightarrow b\bar{b}$ events with high efficiency by using forward proton detector and central calorimeter information. The actual efficiency during a fill will depend on the luminosity profile. If the initial luminosity will go much higher than 10^{34} , as expected in some scenarios, the detector would still require some prescale to meet the allocated bandwidth target. It is anyway foreseen that the detector could not take data during the initial phase (approximately the first hour) of the run, due to possibly unstable beam conditions.

5.1 Trigger rates without forward proton tagging at L1

So far, we have considered the case where a proton is tagged in the 220 detector, assuming that the other will be tagged in the 420 m one, even if this information is not available at trigger level. The acceptance of this asymmetric tagging decreases rapidly with the mass of the central system, and for the light Higgs case (120 GeV) more of the events have both protons tagged in the 420 m detectors; the acceptance for symmetric and asymmetric tagging is 20% and 17% respectively. It is therefore worth examining the trigger rates if no forward proton information is used in the L1 trigger decision, to see if the obvious loss of performance due to the lack of proton tagging can be compensated by the higher acceptance for low-mass Higgs production.

In the case of no proton tagged at 220 m, not only do we lose the rejection factor of 14 (3) at $2 \times 10^{33} \text{ cm}^{-2} \text{ s}^{-1}$ ($10^{34} \text{ cm}^{-2} \text{ s}^{-1}$) from requiring that a proton is tagged in one of the detector stations, but we also lose the rejection provided by correlating the average di-jet rapidity with the proton tag. Table 7 shows the final results assuming no proton information at L1; $\Delta\phi$ is again used as the conservative estimate and f_T as the optimistic estimate.

The final rates at high luminosity are approximately seven times larger than the rates obtained using forward proton information, implying that the subsequent prescale would have to be seven times

L1 item	Rate at 2×10^{33} (kHz)	Rate at 10^{34} (kHz)
J23+J35 + $X_D=1.5 + \Delta\phi > 2.5$	22	111
J23+J35 + $X_D=1.5 + f_T > 0.45$	4.2	21
J20+J40 + $X_D=1.5 + \Delta\phi > 2.5$	18	92
J20+J40 + $X_D=1.5 + f_T > 0.45$	4.2	21

Table 7: The final rate estimate for the exclusivity trigger with no forward proton information, given two different final trigger requirements, $\Delta\phi$ or f_T , as explained in the text.

larger and the (overall) signal efficiency seven times smaller. However, for a light Higgs mass, the situation is somewhat improved because the *non-proton* trigger strategy will also retain symmetric events (i.e. those events with both protons tagged at 420 m). Given the baseline active edges of the AFP detectors, the acceptance for a 120 GeV Higgs boson is 28% and 17% for symmetric/asymmetric events respectively. However, as the mass increases, the acceptance for symmetrically tagged events decreases, whereas the acceptance for asymmetrically tagged events increases. Therefore, the (overall) effect of removing the proton information at L1 is a factor of 2.5 loss in efficiency for a Higgs mass of 120 GeV and a much larger loss at higher Higgs masses.

6 Conclusions

The $H \rightarrow b\bar{b}$ channel is one of the most challenging for the proposed AFP upgrade, due to the low signal cross section and large background. Successful measurements will depend on the implementation of an efficient trigger with low pre-scale. As expected, a di-jet trigger based only on central detectors is not sufficient to keep a reasonably low L1 rate without big prescales, so information from the AFP detector stations will be required in addition to an upgrade of the L1 calorimeter trigger. In particular the following information must be available:

- The forward proton trigger must be able to trigger only on protons that hit the inner 4 mm of the detector station at 220 m. This means that the sensitive triggering area has to be smaller than the active detector, or that some form of segmentation has to be present.
- The L1 calorimeter must be capable of defining new exclusivity criteria, outlined in section 5, using the E_T , η , and ϕ of the two leading jets.

Using those two ideas, it is possible to keep rates down for thresholds that still provide a reasonable efficiency for low-mass Higgs detection. This should be true even up to the highest luminosities for the exclusivity conditions based on angular information. Extremely good, additional, rejection was observed for the exclusivity criterion, f_T , which utilizes the ratio between jet transverse energies and the total scalar sum of transverse energy in the detector. However, further work with (currently unavailable) pile-up samples is necessary to determine the effect of pile-up on the f_T variable at the highest luminosities.

Acknowledgments

We would like to thank Andrew Brandt, Norman Gee and Thorsten Wengler for useful discussions and comments throughout this work.

A Monte Carlo event samples

The PYTHIA di-jet samples used in the analysis were:

```
mc08.005010.J1_pythia_jetjet.recon.A0D.e323_s400_d99_r474
mc08.005011.J2_pythia_jetjet.recon.A0D.e323_s400_d99_r474
mc08.005012.J3_pythia_jetjet.recon.A0D.e323_s400_d99_r474
mc08.005013.J4_pythia_jetjet.recon.A0D.e323_s400_d99_r474
mc08.005014.J5_pythia_jetjet.recon.A0D.e323_s400_d99_r474
mc08.005015.J6_pythia_jetjet.recon.A0D.e323_s400_d99_r474
mc08.005016.J7_pythia_jetjet.recon.A0D.e323_s400_d99_r474
mc08.005017.J8_pythia_jetjet.recon.A0D.e323_s400_d99_r474
```

Note that JX denotes the parton p_T range of each sample i.e. J1 refers to $17 < p_T < 35$ GeV. Thus the samples can be summed together to give good efficiency for a large range of jet transverse energy. The rates were cross-checked with the PYTHIA minimum bias sample:

```
mc08.005001.pythia_minbias.recon.A0D.e306_s400_d99_r474
```

The exclusive sample, used to determine the cut values and efficiencies, was

```
mc08.106065.ExhumeGG_Et35.merge.A0D.e386_s495_r635_t53
```

which is a 10TeV gg sample. However, we expect the results to not be much different for 14TeV Higgs sample because we restricted the central mass to be in the range $110 < M < 140$ GeV. Thus the topology of the di-jets should be approximately correct.

References

- [1] V. A. Khoze, A. D. Martin and M. G. Ryskin, “Prospects for new physics observations in diffractive processes at the LHC Eur. Phys. J. C **23**, 311 (2002) [arXiv:hep-ph/0111078].
- [2] M. G. Albrow and A. Rostovtsev, arXiv:hep-ph/0009336. J. R. Ellis, J. S. Lee and A. Pilaftsis, Phys. Rev. D **71**, 075007 (2005) S. Heinemeyer, V. A. Khoze, M. G. Ryskin, W. J. Stirling, M. Tasevsky and G. Weiglein, Eur. Phys. J. C **53** (2008) 231 J. R. Forshaw, J. F. Gunion, L. Hodgkinson, A. Papaefstathiou and A. D. Pilkington, JHEP **0804** (2008) 090 M. Chaichian, P. Hoyer, K. Huitu, V. A. Khoze and A. D. Pilkington, arXiv:0901.3746 [hep-ph].
- [3] B. E. Cox, F. K. Loebinger and A. D. Pilkington, JHEP **0710** (2007) 090
- [4] The FP420 R&D Project: Higgs and New Physics with forward protons at the LHC. By FP420 R and D Collaboration (M.G. Albrow et al.). FERMILAB-FN-0825-E, Jun 2008. 176pp. e-Print: arXiv:0806.0302 [hep-ex]
- [5] Norman Gee private communication.
See also (for instance) N.Gee’s talk at the latest Rome TDAQ week:
<http://indico.cern.ch/materialDisplay.py?contribId=23&sessionId=4&materialId=slides&confId=56544>

- [6] ATLAS forward detectors for Measurement of Elastic Scattering and Luminosity Determination: Technical Design Report ATLAS-TDR-018 ; CERN-LHCC-2008-004.
- [7] A. Brandt, S. Kolya and J.Pinfeld, in preparation.
- [8] F. Schmidt, P. K. Skowronski and E. Forest, *In the Proceedings of Particle Accelerator Conference (PAC 07), Albuquerque, New Mexico, 25-29 Jun 2007, pp 3381.*
H. Grote and F. Schmidt, *In the Proceedings of Particle Accelerator Conference (PAC 03), Portland, Oregon, 12-16 May 2003, pp 3497.*
- [9] P.Bussey, private communication
- [10] PYTHIA 6.400 manual, published in JHEP 05 (2006) 026 (LU TP 06-13, FERMILAB-PUB-06-052-CD-T, hep-ph/0603175)
- [11] J.Monk, A.Pilkington Comput.Phys.Commun.175:232-239,2006.